ACES Asian Chemical Editorial Society

doi.org/10.1002/asia.202300520

CHEMISTRY AN ASIAN JOURNAL Research Article

www.chemasianj.org

VIP

Fluoride Anions: Unexploited but Effective Halogen Bond Acceptors

Andrea Daolio,[a] Andrea Pizzi,[a] Susanta K. Nayak,[b] Justyna Dominikowska,[c] Giancarlo Terraneo,[a] Pierangelo Metrangolo,[a] and Giuseppe Resnati*[a]

Abstract: Due to their high electron density, fluoride anions can be considered the most effective halogen bond (HaB) acceptors among the halides. However, under common experimental conditions, F^- uncommonly acts as HaB acceptor, expectedly as it is present in hydrated form. Herein we report that under specific crystallization conditions a hydrogen bond-free F^- functioning as donor of electron density can be obtained, with the formed HaBs constituting the driving force of the observed crystal packings. Computations confirm the strength of these HaBs compared to analogous interactions involving other halides.

Introduction

Halide anions (X^-) are effective donors of electron density when interacting with electrophilic halogens, namely they are particularly good halogen bond (HaB) acceptors.[1] The chameleonic ability of halide anions to drive recognition and self-assembly processes via HaB has been investigated extensively in solution[2] and in the solid.[3] In crystals, halides can function as mono- and polydentate HaB acceptor sites, specifically they can form from one up to eight HaBs,[4,5] and supramolecular anionic architectures with very different topologies are formed.

Both calculations and experimental findings indicate that the strength of the HaBs formed by different halide anions is different.[6–8] The electron density is more diffuse on larger halides[9] than on smaller halides so that the electrostatic attraction is weaker in the HaBs formed by larger anions.[6] As revealed by the study of diverse halogen bonded adducts, critical dissociation energies in the gas phase and association constants in solution are smaller when the atomic mass of the halide is greater.[10,11] Fluoride anions afford the strongest HaBs,[12] iodide anions afford the weakest HaBs,[10] and chloride and bromide anions give interactions of intermediate strength.[13] For instance, the computed HaB energies of $FI\cdots X^-$ or $CF_3Br\cdots X^-$ adducts are −75.0, −49.8, −45.1, and 41.9 kcal mol^{-1} or 14.81, 12.76, and 10.68 kcal mol^{-1} when X is F, Cl, Br, and I or Cl, Br, and I, respectively.[11,12]

An analysis of the Cambridge Structural Database (CSD) indicates that the relative frequency of formation of crystalline and halogen bonded adducts starting from different halide anions is opposite to the relative strength of respective HaBs. While some of the obtained datasets are too small to allow for making definite and general statements, the CSD analysis forcefully suggests that iodide anions are the most prone to form HaBs and fluoride anions are the least prone (Table 1).

Many factors such as charge density or polarizability may be considered to describe the chemical behavior of F^- with respect to other halides. Among them, the strength of hydrogen bonds (HBs) formed by different halides and their respective hydration energies are the most suitable in clarifying this seeming contradiction between the strength and the frequency of occurrence of HaB formed by different halides. In fact, the strength of $H\cdots X^-$ HBs decreases when the size of the halide increases, for instance, the computed HB energies for $FH\cdots X^-$ adducts are −53.0, −26.6, −21.9, and −18.1 kcal mol^{-1} when X is F, Cl, Br, and I, respectively.[12] The hydration energies of different halides run parallel to the strength of respective HBs, being the highest for fluoride anions, the lowest for iodide

Table 1. Number of structures in the CSD[a] containing an halocarbon (C–F,Cl,Br,I) and a halide anion (X^-) and number of structures (respective percentage in parenthesis) wherein the two units form an halogen bonded adduct (C–F,Cl,Br,I···X^-).

	$X^- = I^-$	$X^- = Br^-$	$X^- = Cl^-$	$X^- = F^-$
C–F,Cl,Br,I and X^-	861	1282	3467	107
C–F,Cl,Br,I···X^-[b]	306 (35.5%)	330 (25.7%)	307 (8.8%)	5 (4.6%)

[a] ConQuest 2.0.5 was used. [b] I···X^- separation shorter than sum of van der Waals radii of involved atoms; C–F,Cl,Br,I···X^- angle in the range 160°–180°.

[a] Dr. A. Daolio, Dr. A. Pizzi, Prof. Dr. G. Terraneo, Prof. Dr. P. Metrangolo, Prof. Dr. G. Resnati
NFMLab, Department of Chemistry, Materials, and Chemical Engineering "Giulio Natta"
Politecnico di Milano
via L. Mancinelli 7; I-20131 Milano (Italy)
E-mail: giuseppe.resnati@polimi.it

[b] Dr. S. K. Nayak
Department of Chemistry
Visvesvaraya National Institute of Technology
S. Ambazari Rd. Nagpur 440 010, Maharashtra (India)

[c] Dr. J. Dominikowska
Department of Physical Chemistry
University of Lodz
Pomorska Łódź, 163/165, 90-236 Lodz (Poland)

Supporting information for this article is available on the WWW under https://doi.org/10.1002/asia.202300520

anions, and of intermediate value for chloride and bromide anions.[14]

Under common crystallization conditions, fluoride anions are present as strongly hydrogen bonded species, typically as hydrated species, and formation of halogen bonded adducts requires HaB donor for HB donor substitution in the first coordination sphere of the fluoride. Indeed, anhydrous fluoride anion is hardly available[15] consistent with the fact that its hydration energy is as high as 111 kcal mol^{-1} while anhydrous iodide anion is easily accessible as its hydration energy is 66 kcal mol^{-1}.[14] We reasoned that the high energetic cost associated with fluoride anion dehydration and cleavage of other HBs in which it is involved may account for the very low frequency of formation of halogen bonded adducts wherein fluoride anion is the HaB acceptor.

Being interested in preparing halogen bonded cocrystals under control of fluoride anion driven self-assembly, we adopted crystallization conditions which minimize fluoride anion hydration and resulting energetic cost for halogen bonded cocrystal formation. Here we report how these conditions allowed for the preparation of the adducts **4a**, **b** comprised of 1,4,7,10,13,16-hexaoxacyclooctadecane (18-crown-6, **1**), potassium fluoride (**2**), and 1-iodo-heptafluoropropane (**3a**) or 1,4-diiodo-octafluorobutane (**3b**) (Figure 1). Some structural features of these cocrystals confirm that fluoride anions are strong HaB acceptors. The adopted experimental conditions are quite simple and expectedly can be employed easily for other substrates. Several other cocrystals wherein fluoride anion is the HaB acceptor may become available; it will thus become possible to investigate the specific features of fluoride anion in halogen bonded self-assembled systems and to explore the applicative usefulness of halogen bonded cocrystals containing fluoride anions, e.g., as nucleophilic fluorinating agents.[16]

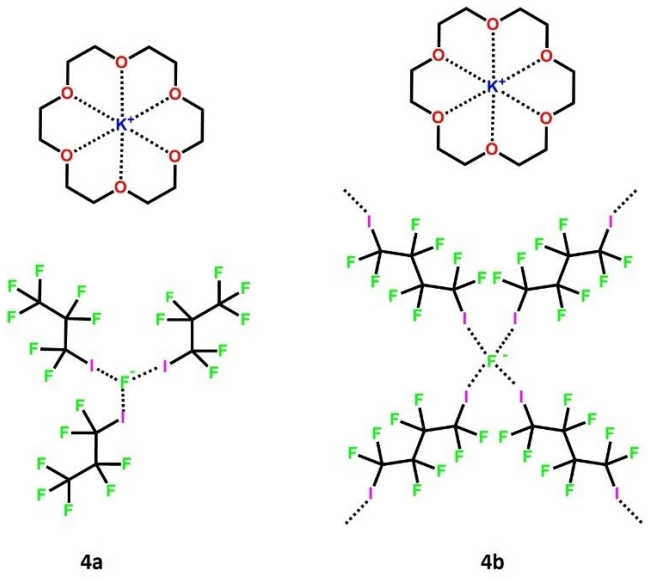

Figure 1. Molecular structure of cocrystals **4a** and **4b**.

Results and Discussion

In the crystal structure of compound **4a** (Figure 2), the most notable close contact, and hence the focus of this discussion, is the one between the iodine atom of 1-iodo-1,1,2,2,3,3,3-heptafluoro propane and the naked fluorine anion from KF. This HaB is as short as 254.3 pm (Nc: 0.76)[17] and displays a very directional F···I–C angle of 178.02°. This interaction is held between a single fluorine atom and three different 1-iodo-1,1,2,2,3,3,3-heptafluoro propanes; the I···F···I angles are 106.45°. The fluoride is also coordinated by one potassium cation, presenting three K···F···I angles of 112.34°. The potassium atom is then coordinated by the six oxygen atoms of the 18-crown-6 molecule. This supramolecular entity made of three 1-iodo-1,1,2,2,3,3,3-heptafluoro propanes, KF and 18-crown-6 is able to assemble in a complex two-dimensional architecture, so that every 18-crown-6 molecule is surrounded by other 1-iodo-1,1,2,2,3,3,3-heptafluoro propane units on the ring plane, in

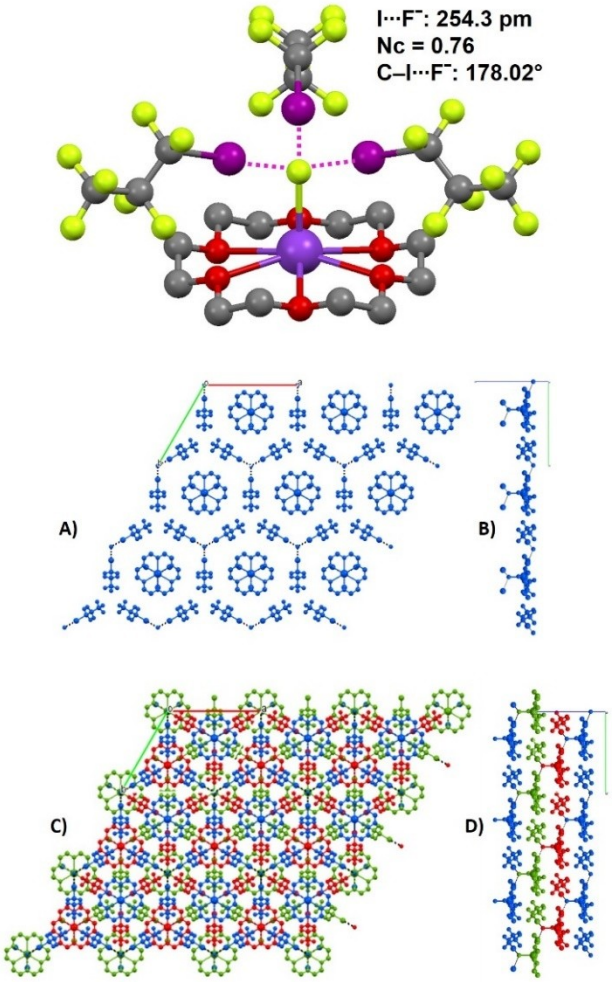

Figure 2. Ball and stick representation of crystal structure **4a** (top). HaBs are depicted as purple dotted lines. Color code: gray, C; red, O; violet, K; yellowish green, F; purple, I. View along crystallographic axes *c* (A and C) and *a* (B and D), of one (A and B) and multi- (C and D) layers present in the crystal packing of **4a**. All units in a layer are in the same color (blue, top layer; red, mid layer; green, bottom layer).

turn engaging in HaB with other F^- anions. It is noteworthy that there are no visible hydrogen bonds between the fluorides (both from the iodoperfluoroalkanes or KF) and the hydrogen atoms of 18-crown-6. In addition, the HaBs seem to be strong enough to overcome the repulsion between the various F···F steric clashes present in the structure between various units of 1-iodo-1,1,2,2,3,3,3-heptafluoro propane.

In the structure of crystal **4b** (Figure 3) the potassium cation is coordinated to two units of 1,4-diiodo-1,1,2,2,3,3,4,4-octafluoro-butane through two fluorine atoms, approaching the cation above and beneath the ring plane. The potassium is then coordinated to ten different atoms. The iodoperfluoroalkanes and crown ether moieties form pillars that extend along the a and c axes of the crystal. The pillars are held together by HaBs between the iodines of 1,4-diiodo-1,1,2,2,3,3,4,4-octafluoro-butane and a naked fluoride anion at a distance of 255.2 pm (Nc: 0.76) with an F···I–C angle of 178.22°. Another two units of 1,4-diiodo-1,1,2,2,3,3,4,4-octafluoro-butane positioned roughly parallel to the pillar engage in an HaB with the fluoride, this time with a separation of 264.6 pm (Nc: 0.79) and an interaction angle of 177.45°. Once again, there are no visible hydrogen bonds between the hydrogens of 18-crown-6 and the 1,4-diiodo-1,1,2,2,3,3,4,4-octafluoro-butane units or the fluoride anions. HaBs are the shortest interactions in both the structures and, lacking any other relevant close contact between the molecules of these two systems, they can be considered to play a major role in the crystals formation.

Compounds **4a**–**b** display perfluorinated iodoalkanes bound to halide anions, similarly to previously reported crystal structures (CSD refcodes GEBCEX and GEBCIB, Figure 4).[18] We decided to investigate these halogen-halide interactions through computations, in order to get a detailed insight into their properties, namely how the nature of the involved halogen atoms affects the features of the occurring HaBs. The NCI method confirms the presence of three (compound **4a**) and four (compound **4b**) strong and attractive HaBs between F^- and iodine atoms of C_3F_7I and $C_4F_8I_2$, respectively (Figure 5).

Further analysis of electron density distribution was based on the quantum theory of atoms in molecules (QTAIM). QTAIM parameters for I···F^- (**4a**–**b**), I···Cl^- (GEBCEX) and I···I^- (GEBCIB and the triiodide anion) contacts are collected in Table 2. The QTAIM properties of I_3^- anion were also considered for comparison as I···I^- contacts in the triiodide anion are considered the strongest known halogen bonds.[19] The order of magnitude of electron density in the studied BCPs (ρ_{BCP}), approximately 10^{-2} au, is typical for halogen bonds,[20] and the positive values of the Laplacian of the electron density allow to classify all I···X^- interactions as showing a closed-shell character. However, partially covalent character of these interactions is confirmed by the two-center delocalization indexes δ(A,B), the

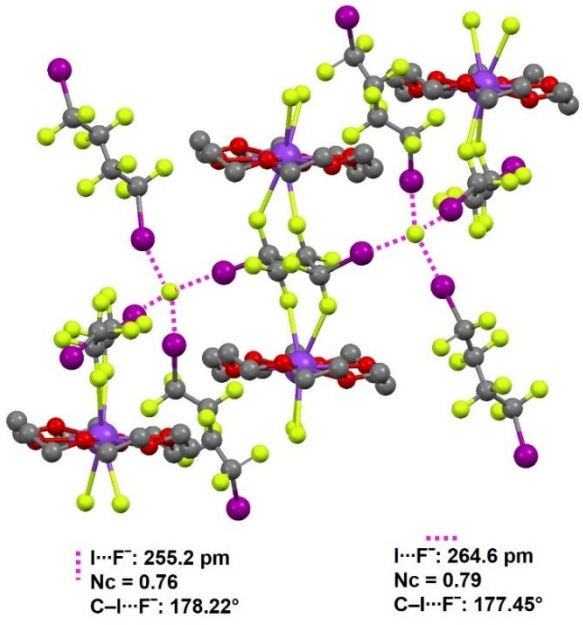

Figure 3. Ball and stick representation of crystal structure **4b**. HaBs are depicted as purple dotted lines. Color code: gray, C; red, O; violet, K; yellowish green, F; purple, I.

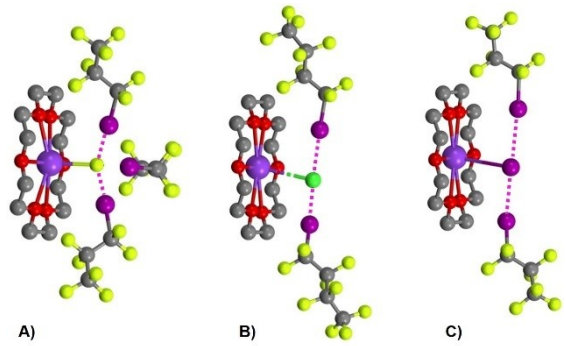

Figure 4. Comparison between crystal structure of compound **4a** (A) with analogues GEBCEX (B) and GEBCIB (C). Halogen bonds are purple dashed lines; color code: gray, C; red, oxygen; violet, potassium; yellowish green, fluorine; green, chlorine; purple, iodine.

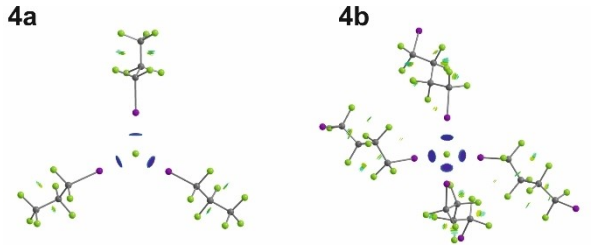

Figure 5. NCI isosurfaces for 4a (left) and 4b (right), colored according to the sign of the second eigenvalue of Hessian of the electron density times the density; blue disks: strong and attractive non-covalent interactions, shallow green sheets: very weak non-covalent interactions.

Table 2. QTAIM parameters at BCPs for I···F, I···Cl and I···I contacts (in au).[a]

Structure	Contact	ϱ_{BCP}	$\nabla^2\rho_{BCP}$	−G/V	δ(A,B)
4a	I···F	0.036	0.139	0.973	0.295
4b	I···F	0.030	0.121	1.025	0.242
GEBCEX	I···Cl	0.030	0.076	0.959	0.395
GEBCIB	I···I	0.022	0.046	1.000	0.398
I_3^-	I···I	0.048	0.047	0.707	0.882

[a] Computed at the M06-2X/x2c-TZVPPall level.

values of which are greater than 0.2 au (the lowest values obtained for I···F⁻ contacts in **4b**) and they increase in order I···F⁻ (**4b**) < I···F⁻ (**4a**) < I···Cl⁻ < I···I⁻. For GEBCEX and GEBCIB δ(A,B) values are almost 0.4 au showing the highest bond order among the studied structures. For comparison for triiodide anion the δ(A,B) value is equal to 0.882 au, indicating that the I···I⁻ contact in I_3^- is much closer to a covalent bond in its character than other investigated contacts. The values of ratio −G/V < 1 also indicate stabilisation due to local concentration of electron density in the BCP. For all studied systems, except of I_3^- showing much greater electron density concentration in the BCP (−G/V = 0.707), this ratio is close to 1.

The condition −G/V < 1 is fulfilled in the case of **4a**, GEBCEX and GEBCIB but in the case of **4b** this ratio amounts to 1.025 and may be attributed to higher number of ligands bound to the fluoride anion, preventing electron density concentration in the I···F⁻ BCPs. It should also be noted that the ratio −G/V increases with the number of ligands bound to the halide anions.

The nature of I···F⁻, I···Cl⁻ and I···I⁻ interactions was further studied using the interacting quantum atoms (IQA) method (Table 3), which decomposes the total energy of a studied system into a sum of atomic self-energies and interaction energies between all atoms of the system. Interestingly, the I···F⁻ interactions in **4a** (−94.9 kcal mol^{-1}) are stronger than the I···I⁻ interactions in I_3^- (−85.8 kcal mol^{-1}). The interactions between atoms in I···F⁻ contacts in **4b** are only 4.8 kcal mol^{-1} weaker than in the triiodide anion. Although the values of interaction energies for I···F⁻ contacts in **4a** and **4b** and I···I⁻ contacts in I_3^- are comparable, their nature is different. Indeed, while the I···I⁻ contacts in I_3^- are dominated by the exchange-correlation component (E_{XC}) and the classical term is practically negligible (0.5 kcal mol^{-1}), I···F⁻ contacts are dominated by the classical component (E_{cl}), the value of which is almost twice the value of the exchange-correlation term. Interestingly, the ratio E_{cl}/E_{XC} diminishes in order: I···F⁻ (**4a** and **4b**), I···Cl⁻ (GEBCEX), I···I⁻ (GEBCIB). The values of E_{XC} for **4a**, **4b**, GEBCEX and GEBCIB show much smaller changes (the difference between its highest and lowest value is 11.8 kcal mol^{-1}) in comparison with the values of E_{cl} (they differ by 41.8 kcal mol^{-1}). This leads to the conclusion that, for the studied structures, the E_{cl} component has much stronger impact on the interaction energies than the E_{XC} term.

For each of the studied systems two interaction energies were calculated. The first one, ΔE_1, is the energy of interaction between a halide anion and all ligands bound to it, divided by the number of ligands (using mean value allows to compare the results obtained for a different number of ligands).

The second one, ΔE_2, is the interaction energy between one of the perfluorinated iodoalkane ligands and the remaining part of the system. The results, not including and including the counterpoise correction (CP) are collected in Table 4.

Mean values of energy of interactions between the halide anions and the ligands bound to them follow the same trend as the IQA energies for atoms forming HaBs. The absolute values of interaction energies (ΔE_1 and ΔE_1^{CP}) decrease in order: **4a**, **4b**, GEBCEX and GEBCIB. Taking this into account, one may conclude that I···F⁻ (in **4a** and **4b**) interactions are stronger than I···Cl⁻ (in GEBCEX structure) and I···I⁻ (in GEBCIB structure) interactions. For ΔE_2 and ΔE_2^{CP} such order is not kept due to the fact that interactions between the ligand and the rest of the system are affected by interactions between the ligands (not identical for each system and arranged around a halide anion in a different manner), and ΔE_1 and ΔE_1^{CP} are free of such an impact by definition.

Conclusions

In the present paper it was demonstrated how uncommon interactions can be transformed into the driving force of a cocrystal formation by getting rid of competing interactions and how this can be obtained by rational and smart design and forecasting of the interaction's strength. To prove this, two crystal structures were obtained, both displaying strong HaBs between an iodine of an iodoperfluoroalkane and a naked fluoride anion. The absence of hydrogen bonds in those structures lead us to infer that these HaBs drive the formation of the observed crystal packings. This paper also reports the reaction's conditions used to obtain the two structures, that can in principle be used to produce peculiar crystals usually hard to obtain with ordinary methods. The same experimental conditions may be used as a new source of naked fluoride anions; this could be important in the synthesis of metal fluoride complexes,[21–24] the latter being of major interest for their unusual reactivity, including C–F bond formation or cleavage and their role as asymmetric catalysts.[25] Computations support our crystallographic findings, revealing that I···F⁻ HaBs are stronger than analogous I···Cl⁻ and I···I⁻ HaBs found in previously reported crystal structures, confirming that fluoride anion is the most efficient halogen bond acceptor among the halides.

Table 3. IQA energies for I···F, I···Cl and I···I contacts (in kcal mol^{-1}).[a] All energetic contributions can be summed in the equation $E_{int} = E_{cl} + E_{XC}$.

Structure	Contact	E_{int}	E_{cl}	E_{XC}
4a	I···F	−94.9	−60.3	−34.7
4b	I···F	−81.0	−53.0	−28.1
GEBCEX	I···Cl	−72.8	−32.9	−39.9
GEBCIB	I···I	−54.2	−18.5	−35.7
I_3^-	I···I	−85.8	0.5	−86.3

[a] Computed at the M06-2X/x2c-TZVPPall level.

Table 4. Interaction energies for all studied systems (in kcal mol^{-1}).[a]

Structure	ΔE_1	ΔE_1^{CP}	ΔE_2	ΔE_2^{CP}
4a	−32.6	−29.2	−19.3	−18.4
4b	−27.1	−24.3	−14.8	−14.1
GEBCEX	−25.6	−23.8	−19.7	−18.8
GEBCIB	−18.3	−18.0	−15.4	−15.2

[a] Computed at the M06-2X/x2c-TZVPPall level.

Experimental Section

Materials: Starting materials and AR grade solvents were purchased from Sigma–Aldrich, TCI (Europe and Japan), and Apollo Scientific and were used without any further purification.

Cocrystals preparation: 132 mg of **1** (0.5 mmol) were heated up under argon until melting occurred and an equimolar amount of powdered and spray dried **2** (29 mg, 0.5 mmol) were added. Excess **3a**, or **3b**, were added under stirring till a homogeneous and clear solution was formed. Small crystals of **4a**, or **4b**, suitable for X-ray analysis were formed on slow cooling of the solution.

Data collection and refinement: The single crystal data of **4a** and **4b** were collected at room temperature with a Bruker SMART APEX II CCD area detector diffractometer, equipped with graphite monochromator and Mo–Kα radiation (λ = 0.71073 Å). Unit cell refinement and data reduction were performed using Bruker SAINT.[26] Structure solutions were performed with Olex2[27] using charge Flipping methods and Fourier analysis and refinement were performed by the full-matrix least-squares methods based on F^2 implemented in SHELXL 2014.[28] Essential crystal and refinement data are reported in SI. Pictures were prepared using Mercury software.[29]

Computational methods: The structures, taken directly from crystals, were optimized at the M06-2X/def2-TZVPP level.[30–32] In order to verify whether stationary points correspond to potential energy surface minima, a frequency analysis at the same computational level was performed. No imaginary frequencies were found. For optimised structures, interaction energies (not comprising system relaxation), also the ones including the counterpoise (CP) correction were calculated. The optimizations, frequency analysis and interaction energies calculations were performed with the Gaussian 16 program.[33] The comparison between geometrical parameters of the experimental and the optimized structures is presented in Figure S1 and Table S4 of the Electronic Supplementary Information. The optimized halogen-halide contacts were observed to be systematically shorter than in the crystal structure with one exception for longer I···F^- in **4b** but in this case equalization of all I···F^- distances took place during the optimization process.

To identify noncovalent interactions in the studied systems the NCI method[34] was employed. The method is based on steep peaks appearing in the reduced density gradient at low densities between weakly interacting atoms. For optimized structures also an analysis of electron density distribution in the framework of the quantum theory of atoms in molecules (QTAIM) was performed.[35] The following QTAIM properties were considered in this study: electron density at bond critical points (ϱ_{BCP}), its Laplacian ($\nabla^2\rho_{BCP}$), total electronic energy density (H) together with its potential (V) and kinetic (G) components and the two center-delocalization index (δ(A,B)), the latter being a measure of number of electron pairs shared by atoms A and B.

The interacting quantum atoms (IQA) method,[36] consistent with the QTAIM space partitioning, was also applied in this study. The IQA method decomposes the total energy of a studied system into a sum of atomic self-energies and interaction energies between all atoms of the system. The latter can be further decomposed into a sum of the classical term (E_{cl}) and exchange-correlation component (E_{XC}). Basis sets using the effective core potential (ECP) approximation, such as def2-TZVPP[31,32] can be used for QTAIM and IQA analysis.[37] To avoid problems with relativistic effects in QTAIM and IQA analysis, the all-electron x2c-TZVPPall[38] and Sapporo-TZP-2012[39] basis sets in conjunction with the relativistic scheme by eliminating small components (RESC) approach[40] were applied to obtain analyzed wavefunctions. The NCI, QTAIM and IQA calculations were carried out with the AIMAll program.[41]

Acknowledgements

G. R. thanks PRIN-2020, project NICE, no. 2020Y2CZJ2. Calculations were carried out using resources provided by the Wroclaw Center for Networking and Supercomputing (grant No. 118) and PLGrid Infrastructure (ACK Cyfronet Krakow Center, Ares).

Conflict of Interests

The authors declare no conflict of interest.

Data Availability Statement

The data that support the findings of this study are available in the supplementary material of this article.

Keywords: Halogen Bond · Fluoride anion · Halogen Bond acceptor · Anhydrous fluoride · Halide anions

[1] P. Metrangolo, F. Meyer, T. Pilati, G. Resnati, G. Terraneo, *Angew. Chem. Int. Ed.* **2008**, *47*, 6114–6127.
[2] J. Pancholi, P. D. Beer, *Coord. Chem. Rev.* **2020**, *416*, 213281.
[3] P. Metrangolo, T. Pilati, G. Terraneo, S. Biella, G. Resnati, *CrystEngComm* **2009**, *11*, 1187–1196.
[4] H. M. Yamamoto, J. I. Yamaura, R. Kato, *J. Am. Chem. Soc.* **1998**, *120*, 5905–5913.
[5] S. V. Lindeman, J. Hecht, J. K. Kochi, *J. Am. Chem. Soc.* **2003**, *125*, 11597–11606.
[6] S. J. Grabowski, *Cryst. Growth Des.* **2023**, *23*, 489–500.
[7] Y. Li, L. Meng, Y. Zeng, *ChemPlusChem* **2021**, *86*, 232–240.
[8] B. Nepal, S. Scheiner, *J. Phys. Chem. A* **2015**, *119*, 13064–13073.
[9] K. D. Sen, P. Politzer, *J. Chem. Phys.* **1989**, *90*, 4370–4372.
[10] M. S. Taylor, *Coord. Chem. Rev.* **2020**, *413*, 213270.
[11] R. D. Walsh, J. M. Smith, T. W. Hanks, W. T. Pennington, *Cryst. Growth Des.* **2012**, *12*, 2759–2768.
[12] L. P. Wolters, P. Schyman, M. J. Pavan, W. L. Jorgensen, F. M. Bickelhaupt, S. Kozuch, *Wiley Interdiscip. Rev.: Comput. Mol. Sci.* **2014**, *4*, 523–540.
[13] H. Wang, W. Wang, W. J. Jin, *Chem. Rev.* **2016**, *116*, 5072–5104.
[14] Y. Marcus, *Biophys. Chem.* **1994**, *51*, 111–127.
[15] K. Seppelt, *Angew. Chem. Int. Ed. Engl.* **1992**, *31*, 292–293.
[16] A. Gaur, N. V. S. Avula, S. Balasubramanian, *J. Phys. Chem. B* **2020**, *124*, 8844–8856.
[17] The "Normalized Contact" Nc for an interaction involving atoms i and j is the ratio Dij/(RvdW,i + RvdW,j) where Dij is the experimental distance between i and j and RvdW,i and RvdW,j are the van Der Waals radii of i and j; if j is an anion, rPj, the Pauling ionic radius of j, substitutes for rvdWj. The values 198 and 136 pm have been used for I and I^-, respectively.
[18] A. V. Jentzsch, D. Emery, J. Mareda, S. K. Nayak, P. Metrangolo, G. Resnati, N. Sakai, S. Matile, *Nat. Commun.* **2012**, *3*, 905.
[19] G. Cavallo, P. Metrangolo, R. Milani, T. Pilati, A. Priimagi, G. Resnati, G. Terraneo, *Chem. Rev.* **2016**, *116*, 2478–2601.
[20] D. J. R. Duarte, G. L. Sosa, N. M. Peruchena, *J. Mol. Model.* **2013**, *19*, 2035–2041.
[21] N. M. Doherty, N. W. Hoffman, *Chem. Rev.* **1991**, *91*, 553–573.
[22] A. C. Castro, M. Cascella, R. N. Perutz, C. Raynaud, O. Eisenstein, *Inorg. Chem.* **2023**, DOI 10.1021/acs.inorgchem.2c04063.
[23] V. Thangavadivale, P. M. Aguiar, N. A. Jasim, S. J. Pike, D. A. Smith, A. C. Whitwood, L. Brammer, R. N. Perutz, *Chem. Sci.* **2018**, *9*, 3767–3781.

[24] S. Libri, N. A. Jasim, R. N. Perutz, L. Brammer, *J. Am. Chem. Soc.* **2008**, *130*, 7842–7844.
[25] W. Sattler, S. Ruccolo, G. Parkin, *J. Am. Chem. Soc.* **2013**, *135*, 18714–18717.
[26] *SAINT*, Bruker AXS Inc., Madison, Wisconsin, USA, **2012**.
[27] O. V. Dolomanov, L. J. Bourhis, R. J. Gildea, J. A. K. Howard, H. Puschmann, *J. Appl. Crystallogr.* **2009**, *42*, 339–341.
[28] G. M. Sheldrick, *Acta Crystallogr. Sect. C Struct. Chem.* **2015**, *71*, 3–8.
[29] C. F. Macrae, P. R. Edgington, P. McCabe, E. Pidcock, G. P. Shields, R. Taylor, M. Towler, J. Van De Streek, *J. Appl. Crystallogr.* **2006**, *39*, 453–457.
[30] Y. Zhao, D. G. Truhlar, *Theor. Chem. Acc.* **2008**, *120*, 215–241.
[31] F. Weigend, R. Ahlrichs, *Phys. Chem. Chem. Phys.* **2005**, *7*, 3297–3305.
[32] K. A. Peterson, D. Figgen, E. Goll, H. Stoll, M. Dolg, *J. Chem. Phys.* **2003**, *119*, 11113–11123.
[33] M. J. Frisch, G. W. Trucks, H. B. Schlegel, G. E. Scuseria, M. A. Robb, J. R. Cheeseman, G. Scalmani, V. Barone, G. A. Petersson, H. Nakatsuji, X. Li, M. Caricato, A. Marenich, J. Bloino, B. G. Janesko, R. Gomperts, B. Mennucci, H. P. Hratchian, J. V. Ortiz, A. F. Izmaylov, J. L. Sonnenberg, D. Williams-Young, F. Ding, F. Lipparini, F. Egidi, J. Goings, B. Peng, A. Petrone, T. Henderson, D. Ranasinghe, V. G. Zakrzewski, J. Gao, N. Rega, G. Zheng, W. Liang, M. Hada, M. Ehara, K. Toyota, R. Fukuda, J. Hasegawa, M. Ishida, T. Nakajima, Y. Honda, O. Kitao, H. Nakai, T. Vreven, K. Throssell, J. A. J. Montgomery, J. E. Peralta, F. Ogliaro, M. Bearpark, J. J. Heyd, E. Brothers, K. N. Kudin, V. N. Staroverov, T. Keith, R. Kobayashi, J. Normand, K. Raghavachari, A. Rendell, J. C. Burant, S. S. Iyengar, J. Tomasi, M. Cossi, J. M. Millam, M. Klene, C. Adamo, R. Cammi, J. W. Ochterski, R. L. Martin, K. Morokuma, O. Farkas, J. B. Foresman, D. J. Fox, *Gaussian 16, Revis. C.01, Gaussian, Inc., Wallingford CT* **2016**.
[34] E. R. Johnson, S. Keinan, P. Mori Sánchez, J. Contreras García, A. J. Cohen, W. Yang, *J. Am. Chem. Soc.* **2010**, *132*, 6498–6506.
[35] R. F. W. Bader, *Chem. Rev.* **1991**, *91*, 893–928.
[36] M. A. Blanco, A. Martín Pendás, E. Francisco, *J. Chem. Theory Comput.* **2005**, *1*, 1096–1109.
[37] D. Tiana, E. Francisco, M. A. Blanco, A. Martín Pendás, *J. Phys. Chem. A* **2009**, *113*, 7963–7971.
[38] P. Pollak, F. Weigend, *J. Chem. Theory Comput.* **2017**, *13*, 3696–3705.
[39] T. Noro, M. Sekiya, T. Koga, *Theor. Chem. Acc.* **2012**, *131*, 1–8.
[40] T. Nakajima, K. Hirao, *Chem. Phys. Lett.* **1999**, *302*, 383–391.
[41] T. A. Keith, *AIMAll (Version 19.10.12)*, Overland Park KS, USA, **2019**.

Manuscript received: June 12, 2023
Revised manuscript received: July 3, 2023
Accepted manuscript online: July 8, 2023
Version of record online: July 20, 2023